Metal-Organic Framework Composites

Syed Shoaib Ahmad Shah, Tayyaba Najam, and Hai-Long Jiang

Contents

Introduction 2
Synthetic Protocols for MOF Composites 3
Solvothermal/Hydrothermal Synthesis 4
Coprecipitation Synthesis 5
Microwave Synthesis 6
Surface Encapsulation 8
In Situ Synthesis 9
MOF Composites 11
Organic Matrix-MOF Composites 12
Inorganic Matrix-MOF Composites 18
Conclusion 25
Cross-References 25
References 26

Abstract

Metal-organic framework (MOF)-based composites have been developed to integrate respective features of the two materials toward diverse applications. The characteristic features of MOFs can be translated into MOF composites with additional properties including the stability, conductivity, and functional active sites. Herein, synthesis methods used to produce MOF composites and current developments in MOF composites for various applications have been

S. S. A. Shah
Department of Chemistry, School of Natural Sciences, National University of Sciences and Technology, Islamabad, Pakistan

T. Najam
Institute of Chemistry, The Islamia University of Bahawalpur, Bahawalpur, Pakistan

H.-L. Jiang (✉)
Hefei National Research Center for Physical Sciences at the Microscale, Department of Chemistry, University of Science and Technology of China, Hefei, Anhui, P. R. China
e-mail: jianglab@ustc.edu.cn

© Springer Nature Singapore Pte Ltd. 2025

X.-H. Bu, S. Ma (eds.), *Handbook of Metal-Organic Frameworks*,
https://doi.org/10.1007/978-981-99-8242-4_18-1

summarized. Additionally, the ways in which MOFs counteract with different substrates to produce functional materials for different applications were thoroughly examined, highlighting the MOF composites not only as promising materials but also as unique solutions to the rising problems of modern society.

Keywords

MOFs · MOF composites · Functional NPs@MOF · Enzymes@MOFs · Carbon@MOFs · MOF@MOF

Introduction

Metal-organic frameworks (MOFs) have sparked interest because of their unique features as potential functional materials with remarkable physical and chemical characteristics, intriguing porosity structures, and ease of functionalization [1]. These crystalline/definite porous materials with consistent high surface areas (1000–10,000 m^2/g) and pore size are surpassing other porous materials including chitosan, activated carbon (AC), zeolites, and silica. MOFs have exclusive qualities such as unified dimensional frameworks (1D, 2D, and 3D), high porosity, customizable crystal structure, precise networks, and different geometries that may be employed for a variety of uses [2]. Nevertheless, flaws of MOFs posed significant challenges in their vast range of applications. As a result, effort has been directed toward post-synthetic modification of MOFs in order to attain the necessary characteristics; in some circumstances, such MOFs are flawed, compromising their structural foundation and analytical performance. The low electrical conductivity and weak stability in harsh environment are the major drawbacks in wide applications of pristine MOFs [3]. There are several ways to overcome these drawbacks; for example, hydrophobic coating on surface enhances the water stability of MOFs by protecting metal-ligand bond from hydrolytic attack [4], and resistance to chemical degradation is induced by using functional group linkers; this resistance in turn improves the mechanical stability of MOFs [5]; aperiodic network topology is also used to increase elastic stability without adding to the MOF density or decreasing porosity [6]; sometimes, defects are deliberately created in MOFs to benefit certain property like adsorption [7], and post-synthetic modification (PSM) is also used to tune properties and increase stability of MOFs [8]. However, the precise combination of MOFs with other functional materials, both materials retained their characteristics features, is an emerging and efficient strategy to improve the functionality [9]. These MOF-based composites were created using immobilization, surface modifications/functionalization, impregnation, as well as deposition processes [10]. More or less, these approaches were capable of producing MOF composites with superior characteristics, making them interesting materials for a wide range of applications, where their distinctive characteristics may be adjusted to specific requirements, gas-related processes, adsorptions, and catalysis. MOF composites formed with efficient counterparts/materials have been recommended to improve the typical qualities of MOFs for a

particular use. Thus, several types of MOF composites, such as MOFs with functional nanoparticles, carbon-based materials, as well as other guest materials, have shown more efficacy in respective applications as compared to their pure counterparts. The improved performances have been attributed to the alterations in the surface porosity, efficacy in light absorption, and chemical/mechanical/thermal stability in the MOF composites. These MOF composites have shown enhanced stability without compromising on porosity [11], superior electrical conductivity [12], easily customized surface area for required application through careful selection of secondary material [13], and a range of secondary materials make MOF composites applicable in versatile areas [14], giving them an edge over the other materials in dealing with drawbacks of pristine MOFs. It is often used for any intended future of MOFs. Recent work on MOF composites shows trends are moving not only toward better performance but also toward more sustainability and economic options. Zaman et al. prepared Fe-based MOF composite as an alternative to precious metal-based electrocatalyst for methanol oxidation in direct methanol fuel cells [15]. Li et al. developed g-C_3N_4 with Zn-MOF (CN/Zn-MOF) nanosheet photocatalyst through microwave-hydrothermal method. It showed high conduction even at lower temperature and rapid charge transfer degrading tetracycline (TC) into eightfold more H_2O_2 than precursor MOF [16]. Zhu et al. prepared Si@Mn-MOF composite which deal with volume expansion problem of Si anode in Li-ion batteries (LIBs). It showed improved electrochemical performance and reversibility, suggesting the convenient use of Si reserves in LIBs, keeping cost factor under control [17].

Synthetic Protocols for MOF Composites

The creation of MOF-based functional composites with particular qualities has been extensively researched due to the growing need for conductivity, catalysis, and other applications. Generally speaking, the kind of metal, organic linker, and targeted support/host/guest dictate the synthesis approach for MOF composites. MOF composites with distinct structures and characteristics may be produced by synthesis beginning with the same reaction initiators but changing the synthesis approach. The morphology, crystal structure, and porosity of MOF composites may be significantly impacted by the synthesis process and particular experimental circumstances, which will further impact their functionalities [18]. Strong external energy must be used during MOF composite synthesis in order to encourage the development of a framework structure. MOF composites with various characteristics have been prepared via solvothermal, microwave, ultrasonic, and electrochemical techniques. Functional nanoparticles (NPs) like carbon dots, magnetic NPs, metal oxides, and enzymes are integrated into MOFs to prepare MOF composites. This permits the materials to retain high porosity and multichannel structures while allowing for structural and functional modification [19]. This synthesis technique was employed by Feng et al. to create stable bimetallic CoFe-MOF-graphene composites. The electrical signal was significantly enhanced by the combination of graphene's exceptional electrical conductivity, high specific surface area, and tunable porosity [20].

Solvothermal/Hydrothermal Synthesis

A methodical approach to creating MOFs and related composites is solvothermal synthesis. This method requires little pressure, works at low temperatures, and has good yield potential. In solvothermal processes, choosing the right solvent for a given reaction is essential. Several organic solvents are suitable for the synthesis of MOF composites including N, N-dimethylformamide (DMF), N, N-diethylformamide (DEF), toluene, dimethyl sulfoxide (DMSO), etc. The organic solvents may act as means to guide the production of structures in addition to promoting the creation of new materials. These organic solvents may also act as agents for guiding structure creation, in addition to encouraging the synthesis of new materials. DMF is favored solvent for synthesizing MOF composites due to good solubility and high boiling point. For example, PCN-624 (metalloporphyrin) MOF with functionalization of perfluoro-phenylene was produced using DMF at 120 °C for 72 h [21]. Wu et al. employed this technique to improve PCN-221(Fe_x) solubility in various iron (Fe) concentrations and encapsulated the $MAPbI_3$ QDs into the pores of PCN-221(Fe_x) via a sequential deposition approach. The prepared PCN-221(Fe_x) was submerged in a PbI_2 solution to produce PbI_2@PCN-221(Fe_x). After washing with ethanol, MAI ethanol solution was added to produce the final $MAPbI_3$@PCN-221(Fe_x) composite (Fig. 1a) and used for reduction of CO_2 using $MAPbI_3$/PCN-221(Fe_x) as efficient photocatalyst [22]. Further, Badhulika et al. [23] developed a one-step solvothermal approach for producing MOF-altered NF and as synthesized Ni-MOF/NF composite displayed an extraordinary performance. The resultant MOF composite showed great robustness, and change in conditions did not affect its working; further, this method expanded the life cycle of MOF, and it showed five cycles of catalytic ability without any degradation. The Ni-MOF nanosheets and NF interacted, resulting in a higher voltage density at the electrode. This is due to NF's ability to permit fast electron transit while also demonstrating significant electrical conductivity at the electrode-electrolyte interface. Catalysts' electrocatalytic activity is boosted by porous nature and the existence of significant charges caused by nodes vacancies. Several studies have also proven the efficiency of solvothermal method for the synthesis of MOFs and their composites in a variety of lengths, widths, and morphologies.

The hydrothermal synthesis approach may also be used to produce MOFs and MOF composites [25]. The hydrothermal technique permits for temperature, reaction time, precursor, solvent, and pH variations. By adjusting the synthetic conditions, the size of particles (MOF composites) may be easily tuned. Several teams have employed the hydrothermal reaction technique to synthesize MOFs and composite materials with remarkable performance [26]. For example, Du et al. [27] synthesized the NH_2-UiO-66 and its composite with ZnO (ZnO/UiO-66-NH_2) by a hydrothermal method. After stirring for 2 hours in deionized water, a combination of $ZnAc_2$ and NH_2-UiO-66 shaped like NPs was effectively converted into the ZnO/NH_2-UiO-66 composite. Similarly, MIL-101(Cr)-Ag composite was produced successfully by combining MIL-101(Cr) with Ag NPs [28]. During the hydrothermal process, the ratios in the precursors may be altered to yield MIL-101(Cr) with

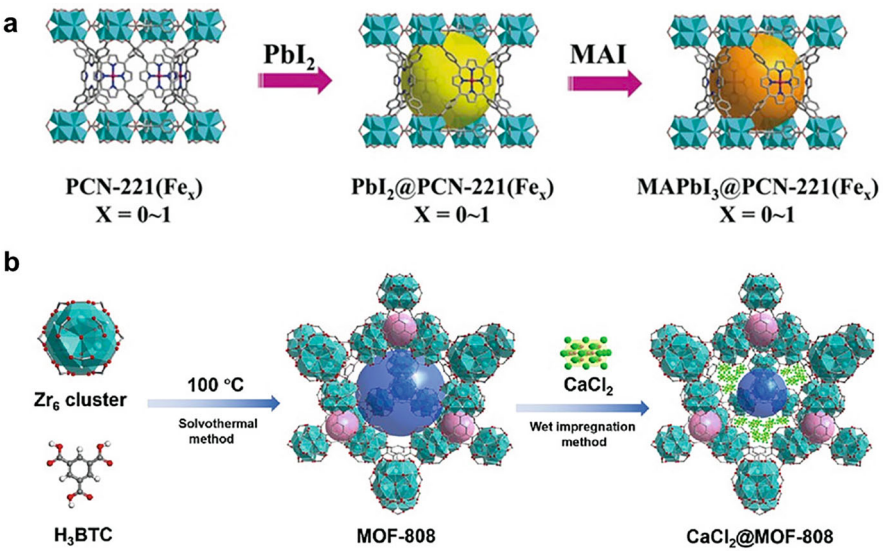

Fig. 1 Schematic representation of MOF composites. (**a**) Solvothermal synthesis of $MAPbI_2$@PCN-221(Fe_x) composite. (Reproduced from Ref. [22]). (**b**) Controlled synthesis of MOF-808 and $CaCl_2$@MOF-808 composite. (Reproduced from Ref. [24] Copyright Elsevier @2023)

diameters ranging from 80 to 800 nm. The controlled hydrothermal synthesis process called modulated hydrothermal (MHT) production was reported, which produced excellent MOF-808(Hf). This MOF is made from 1,3,5-benzene tricarboxylic acid (BTC) and hafnium tetrachloride [29]. The hydrothermal process was used for the synthesis of MOF-808 composite with $CaCl_2$ (Fig. 1b), which revealed the efficiency of method for the development of composites of ionic salts within pores of MOFs [24]. The wet impregnation method was used by adding $CaCl_2$ in the suspension of MOF-808 in water, and the contents of $CaCl_2$ in the $CaCl_2$@MOF-808 composite can be tuned by varying the ratio of $CaCl_2$ and MOF-808. The hydrothermal procedure is the most effective way for synthesizing MOFs and MOF composites, and it also allows for simple size adjustment. The hydrothermal reaction technique allows for the simple modification of the size of MOFs and MOF composites without compromising their high-quality output requirement [26].

Coprecipitation Synthesis

An established technique for creating inorganic NPs is solution precipitation, an additional process where cations precipitate simultaneously is the coprecipitation method. MOFs and their composites can be synthesized more quickly and easily using the solution precipitation technique than the hydrothermal method, which calls for more intricate steps and harsher reaction conditions. Sun et al. [30] using this

technique synthesized ZIF-67 and produced crystals with a variety of shapes, such as pitaya-like, rhombic dodecahedral, and leaf-like structures. This study revealed that the morphology of ZIF-67 can be tailored by varying the solvent used during synthesis. Utilizing deionized (DI) water as the solvent results in leaf-like morphology. When methanol is employed as the solvent, ZIF-67 adopts a rhombic dodecahedral morphology. Moreover, a pitaya-like morphology was attained by using a mixture of both solvents (DI water and methanol). In recent years, coprecipitation method for the synthesis of MOFs has also extended significantly for the synthesis of MOF-based composites [31]. For instance, Chen et al. [32] synthesized Ru-NH_2-UiO-66/Mn composites using coprecipitation as well as solid-state mixing methods. In the solution precipitation process, Ru precursor and NH_2-UiO-66 were dissolved in DI water and stirred continuously. Subsequently, manganese dioxide (MnO_2) was hosted into MOF, leading to the formation of the Ru-NH_2-UiO-66/Mn composite. Similarly, Choi et al. [33] reported the fabrication of Ren-MOF composites using the solution precipitation method. During the synthesis, precise control and adjustment of temperature enabled the production of MOF-based composites with varying morphologies and dimensions.

Microwave Synthesis

The microwave-assisted synthesis method became more popular as a highly effective method for generating useful nanomaterials. Throughout chemical process, the electromagnetic irradiation frequency usually ranges from 0.2 to 300 GHz. Compared to solvothermal/hydrothermal processes, microwave-based approach is faster and safer. With the advantages mentioned above, this method is frequently employed by numerous researchers to create MOF-based composites [34]. For instance, Nasiri et al. [35] created a magnetically separated MOF composite made of nano$CoFe_2O_4$ and methylcellulose (MC). The one-of-a-kind structure was created utilizing a straightforward, effective, and creative microwave method. The photocatalytic (PC) performance of nano$CoFe_2O_4$/MC was assessed by investigating its efficiency in degrading pollutants under varying experimental conditions. To synthesize nano-$CoFe_2O_4$/MC, $FeCl_3{\cdot}6H_2O$, $CoCl_2{\cdot}6H_2O$, and MC were dissolved in distilled water as the solvent and vigorously stirred at room temperature. Sodium hydroxide (NaOH) was gradually added over 1 h to adjust the pH to 13. The reaction mixture, characterized by its deep brown color, was exposed to microwave irradiation, resulting in the formation of nano$CoFe_2O_4$/MC as a lightweight, dense powder. Resultant nano$CoFe_2O_4$/MC MOF composite explained that microwave-assisted method of synthesis can enhance certain properties of pristine MOF, as one under study showed great degradation ability with high stability and slow aging. This method is also useful to develop MOF composites with great sensing abilities. Xu et al. reported the development of a photocatalyst designated as Fe-UiO-66, highlighting similar innovative approaches in material synthesis. UiO-66 was synthesized by dissolving 2,5-dihydroxyterephthalic acid (H_2BDC) and zirconium tetrachloride ($ZrCl_4$) in a solvent mixture of dimethylformamide (DMF) and acetic

acid (HOAc). The solution was subjected to hydrothermal treatment at 120 °C for 24 hours to facilitate crystallization. To incorporate Fe^{3+} ions into the UiO-66 framework, $FeCl_3 \cdot 6H_2O$ and the synthesized UiO-66 were combined and subjected to microwave irradiation at 85 °C, enabling a rapid and efficient integration of iron ions into the structure (Fig. 2a). Fe-UiO-66 was efficaciously synthesized in 30 min, with the incorporation of Fe^{3+} ions into the Fe-UiO-66 framework facilitated by microwave irradiation. This method ensured the absence of any extraneous nanoparticles beyond the Fe-based unit. Titanium dioxide (TiO_2) is widely recognized as an effective cocatalyst due to its exceptional chemical and physical properties. To enhance the photocatalytic activity of NH_2-UiO-66, a TiO_2/NH_2-UiO-66 composite (t/NH_2-UiO-66) was developed using a microwave-assisted technique. Researchers opted to synthesize the TiO_2/NH_2-UiO-66 composite through two distinct approaches [36]: (i) create a homogenous solution by first mixing the precursors utilized for the synthesis, namely, TiO_2 and NH_2-UiO-66, and (ii) microwave-irradiate it for an hour at 80 °C (Fig. 2b). To improve their PC performance, they used thermally treated TiO_2 (T/NH_2-UiO-66) in place of the titanate precursor in their TiO_2/MOFs composites.

Because of its affordability, the sonochemical method has been established for efficient production of MOF composites owing advantages, including operational safety, environmental sustainability, and the capability to maintain low temperatures [38]. In order to promote energy transfer, sonication synthesis frequently entails the creation and subsequent dissolution of bubbles in the solvent. For example, scientists may be able to create a new structure more easily if they employ sonication to induce new chemical reactions. Numerous studies have been created based on MOFs and MOF composites using the sonication technique [39]. To break down 4-nitrophenol, composite photocatalysts made of g-C_3N_4/Ti-MIL125-NH_2 were synthesized by dispersing the g-C_3N_4 powder in a methanol and DMF mixture [39]. Hlophe et al.

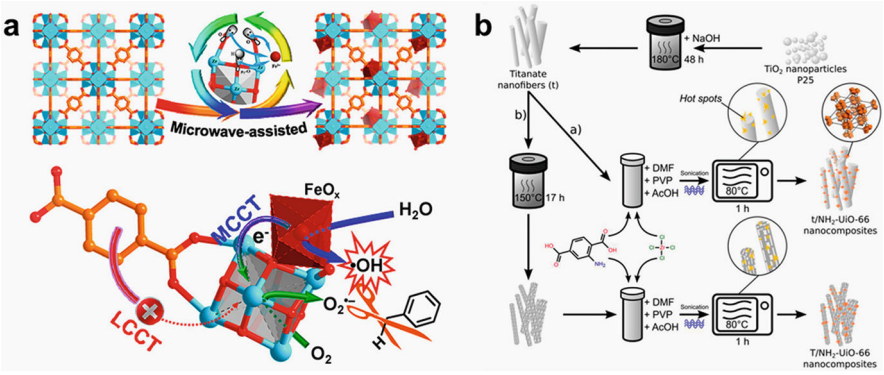

Fig. 2 Microwave-assisted synthesis of MOF composites. (**a**) Preparation of polyhedral Fe-UiO-66. (Reproduced from Ref. [37]). (**b**) Synthesis of TiO_2 and NH_2-UiO-66 composite. (Reproduced from Ref. [36] © 2019 The Authors. Small published by WILEY-VCH Verlag GmbH & Co. KGaA, Weinheim)

[40] used a sonication technique to make a composite out of MIL-125(Ti) and MIL-125(Ti)/black phosphorous (BP) composites. In this study, titanium isopropoxide and 1,4-benzenedicarboxylic acid were used as precursors to manufacture MIL-125 (Ti). Han et al. [41] successfully created monolayer Ni MOFs composite by employing the traditional sonication approach. Using a straightforward combination of BDC precursors, 2-methylimidazole, triethylamine (TEA), and $NiCl_2 \cdot 6H_2O$, ultrasonication for 8 hours produced a high-quality product without the need of surfactant. In the (200) plane, these octahedra are subsequently connected to one another at the corners or edges, creating 2D metal layers that are identified by BDC materials. In addition, after the sonication process, a freezing method (with water help) was used to stop monolayer Ni MOFs from aggregating. Multilayer MOF composites can be sonicated to identify potential high-performance photocatalysis applications. Multilayer MOF composites are among the several morphologies that may be created using the sonication technique. In a similar way, Zhao et al. [42] combined sonication and carbonization to effectively produce polyhedral ZIF-8-derived ZNG composite, after producing the polyhedral ZIF-8 with an ultrasonication technique. Ultimately, polyhedral ZNG composites of various sizes were created.

Surface Encapsulation

Two steps make up the encapsulation process, also referred to as the "build-bottle-around-ship" approach: (i) resynthesized NPs develop MOF shells; and (ii) NPs with uniform size, shape, and structure are created. It is more common to employ MOF self-nucleation and huge lattice structure barriers rather than creating structures that enclose MOFs. Bridges made of flexible materials have been used to address these difficulties. To lessen the lattice difference between NPs and MOFs, the surfactants cetyltrimethylammonium bromide (CTAB) and polyvinylpyrrolidone (PVP) were employed. MOF nucleation on the NP surface might be aided by these organic surfactants. Furthermore, to alter NPs and produce MOF structures, metal hydroxides or oxides may be used. MOFs shells can contain NPs of different sizes thanks to encapsulation. MOF nucleation on the NP surface could be aided by these organic surfactants. Furthermore, to alter NPs and produce MOF structures, metal hydroxides or oxides may be used [43]. NPs of all shapes and sizes can be found in MOF shells thanks to encapsulation. NPs, carbon compounds, enzymes, molecular catalysts, and other useful materials may be inserted into MOF cavities using this technique. Using a bioinspired encapsulating reconfiguration strategy, Feng et al. [44] demonstrated how to create highly hydrophobic mesoporous MOF complexes by carefully altering the outermost layer of a restructured mesoporous MOF network. Hydrophobic alkyl chains that respond by clicking interactions first modify the topmost layer of an insufficient MOF, AlTz-53, which has decreased porousness. When the solvent is eliminated, the internal structure undergoes lattice rearrangement, which significantly increases the material's crystal structure and inner porosity. The natural process of turning from a silkworm into a moth involves a number of activities, such as spinning and changing while enclosed in a protective

shell. This biological phenomenon has inspired researchers to propose an encapsulating reconfiguration method for adding ultimate hydrophobicity to mesoporous MOFs (Fig. 3) [44].

Due to dispersion limits brought on by the structure's small pore size and the relatively large alkyl chain dimensions, the hydrophobic components are altered on the outermost layer of the structure. Researchers have proposed utilizing a click chemistry approach to enhance the hydrophobic properties of AlTz-53. This method involves a deliberate interaction between tetrazine dicarboxylate units present in AlTz-53 and hydrophilic alkenyl-based materials. By introducing large alkenyl compounds, such as 1-octadecene (C18), the microporous metal-organic framework (MOF) surface is modified as these compounds gradually infiltrate the internal pores. The tetrazine subunits undergo rapid and mild click chemistry reactions with alkenyl, alkyne, ketone, or aldehyde functional groups through the inverse-electron-demand Diels-Alder (iEDDA) reaction mechanism. Specifically, the interaction between tetrazine and C18 occurs via the iEDDA pathway, resulting in successful surface functionalization, this approach facilitates the synthesis of an Al-based metal-organic framework (Al-MOF) with dihydropyridazine groups seamlessly incorporated into its fundamental structure. Subsequently, through a "click" reaction mechanism, the tetrazine linkage reacts with alkenyl derivatives, enabling the chemical modification of the AlTz-53 material, which possesses minimal porosity. Upon solvent desorption, the transformation from AlTz-53-C18 to AlTz-68-C18 is successfully achieved.

In Situ Synthesis

Another method for engineering MOF composites is the "ship-in-a-bottle" approach. By putting desirable materials into the cavities of MOFs including chemical

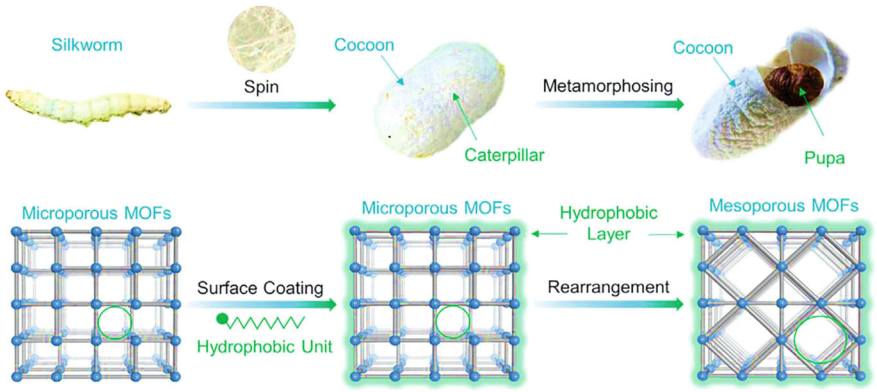

Fig. 3 Bioinspired encapsulating reconfiguration strategy to create highly hydrophobic mesoporous MOF composites. (Reproduced from Ref. [44] © 2020 The Author(s). Published by Elsevier Inc.)

reduction, photoreduction, etc., this method modifies the MOF framework structurally. This synthetic approach has the drawback of not preventing the growth of integrated components on the MOF matrix surfaces. The researchers developed a double-solvent method that ensures all precursors will enter MOF cavities. Li et al. [45] produced a very effective composite called Zr-MOF-s(Pt)(Zr/Ti)-R by employing metal groups to increase the charge carrier transfer rate and MNPs cocatalysts to increase the separation yield. This was accomplished by creating low-sized Pt NPs inside internal spaces and replacing a portion of the Zr(IV) in Zr-based MOF with Ti(IV). The novel catalyst may simultaneously improve H_2 production performance when combined with the previously discussed synergy approach. A dual solvents method was employed to promote the formation of cadmium sulfide (CdS) within the MIL-101(Cr) structure (Fig. 4a) [46]. This encapsulation strategy is particularly useful to impart super-hydrophobicity in MOFs, making composites excel in oil/water separation. Surface encapsulation also makes composites suitable for bio-applications. The potential of the CdS/MIL-101(Cr) to decrease CO_2 was studied in order to assess its efficiency. In comparison to virgin CdS and MIL-101(Cr), the CdS/MIL-101(Cr) combinations demonstrated noticeably higher efficiency in the PC reduction of CO_2. Additionally, it appears that NPs in MOF cavities are uniformly smaller, which is advantageous for possible uses. In situ reactions occurring within the cavities of MOFs, which act as confined

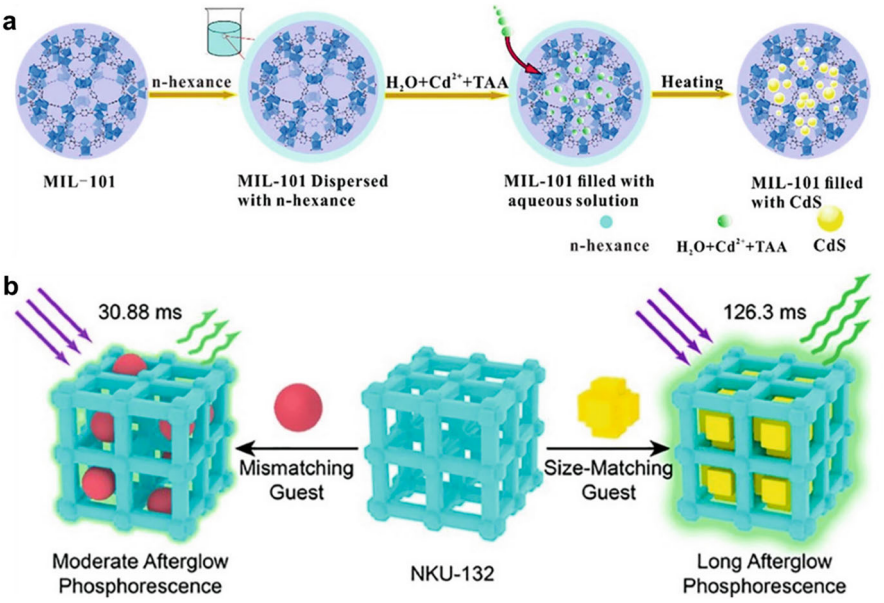

Fig. 4 (**a**) Synthesis of CdS within the MIL-101(Cr) framework to produce MIL-101@CdS composite. (Reproduced from Ref. [46]). (**b**) Host-guest connections, the microporous cavities or channels in MOFs to control over the RTP functioning. (Reproduced from Ref. [50] Copyright © 2021, Science China Press and Springer-Verlag GmbH Germany, part of Springer Nature)

nanoreactors under mild conditions, may readily produce NPs with specific shapes and compositions [47–49]. Using ZIF-8 cavities as a restricted template, PdZn NPs were synthesized by the co-reduction method [47]. In situ method synergistically added counter material to MOF, imparting rapid charge separation and transfer which results in increased photocatalytic activity and NO removal.

Nevertheless, there are still some drawbacks to in situ generation. For example, MOF templates may partially disintegrate as a result of the growing quantity of embedded components. The intricate surface architecture, morphology, and density of embedded materials often present challenges in achieving a comprehensive indulgent in establishing structure-activity relationship in MOF composites. The microporous cavities or channels within MOFs, facilitated by host-guest interactions, offer an additional layer of control over RTP functionality, enabling tailored photophysical properties (Fig. 4b) [50].

The functional performance of MOF composites is highly dependent on the precise regulation of encapsulation conditions for materials integrated into the MOF matrix, particularly in applications such as catalysis and sensing. Despite significant efforts, the development of universally applicable synthesis strategies for diverse nanoparticle/MOF (NP/MOF) composites remains a challenging task. The self-sacrificial template method has emerged as a promising approach due to its robust reaction mechanism and relatively slow kinetics, making it advantageous for the fabrication of hollow nanostructures or core-shell architectures [41]. Critical factors in employing the self-sacrificial template technique include the choice of materials, reaction conditions, and the controlled release rate of metal ions from the template. For instance, ZnO nanorods serve both as structural templates and zinc sources for the development of shells in metal oxide/MOF composites, which can be synthesized using this method [51, 52]. This versatile technique is applicable for the synthesis of metal oxides as well as metal NPs, further enhanced its popularity and simplicity. A notable example of this approach involves the production of composite containing nickel oxide (NiO) on a nickel-based MOF (Ni-MOF). This Ni-MOF/NiO composite was successfully prepared using solvothermal method combined with high-temperature annealing, showcasing the efficacy of the self-sacrificial template technique in creating advanced NP/MOF composites [53]. When NiO nanostructures are applied to the hexagon Ni-MOF, they improve redox reactive sites and electric conductivity while also preventing NiO nanostructure aggregation (Table 1).

MOF Composites

Multicomponent materials, referred to as composites, are composed of multiple distinct nongaseous phase domains, with at least one phase being continuous. These composites leverage the combined properties of all constituent phases, enabling the tailoring of material characteristics to achieve desired functionalities, and they are often utilized in industrial operations. MOFs-based composites have been researched for several applications, including to enhance gas sorption

Table 1 Comparison of different synthesis strategies of MOF composites

Synthesis method	Advantages	Disadvantages	Applications
Solvothermal	Distinct morphology and high crystallinity	Time taking, so more energy is consumed	Catalysis and gas adsorption
Hydrothermal	Give controlled particle size under mild conditions	Crystallinity is average or low	Water treatment and drug delivery
Coprecipitation	Takes less time and efforts, and scalable	No or less control on size and morphology	Capturing carbon dioxide and sensing applications
Microwave-assisted	Give small particles in short time, use less energy, and heat uniformly	Scalability is tough; special apparatus is needed	Photocatalysis and photocatalytic Energy conversion and storage
In situ synthesis	Integrate guest species in controlled way boasting the stability	Minor change in reaction conditions alters the products	Hybrid nanostructures and catalysis
Surface encapsulation	Best for hybrid composites with facility of tuning properties Stable due to ultra-hydrophobicity	Surface engineering is needed which makes it complicated	Drug delivery and catalysis in biological environment

characteristics, gas separation, catalysis, energy storage, sensors, water harvesting/treatment. Furthermore, compared to crystalline MOFs, treating composites is frequently simpler. Composites are particularly interesting in catalysis because they combine the better durability of the continuous phase with the catalytic activity of the dispersed phase, making catalyst recovery simple [54]. By exploring the design principles underlying various MOF composites, it is possible to develop targeted materials with specific structures and properties tailored for a wide range of applications. For instance, MOF composites have been used in energy storage devices [55]; Co-PBA@MXene hybrids showed high conductivity and stability, large surface area, and increased charge separation ability, making them next-generation anodes [56]. Zhang et al. used machine learning and prepared a model for the synthesis of MOF composite and derivatives. The model elaborates phase transformations of Prussian blue analogue (PBA) which are complemented by characterization techniques. Composite prepared using the model exhibited high OER efficiency, suggesting the success of model and its future implementation in material synthesis [57].

Organic Matrix-MOF Composites

Composites made of MOF crystals with an organic matrix were created by using both natural and synthetic materials. For instance, a MOF composite with a monolithic structure was reported, where 4-vinylbenzyl chloride and divinylbenzene were

polymerized to form a macroporous hydrophilic polyHIPE. HKUST-1 crystals were incorporated into the interconnected voids of the monolith by treating the activated polyHIPE with a reaction mixture containing the metal precursor and ligand, followed by a solvothermal reaction [58]. The presynthesized crystals were initially combined with a plasticizer and a liquid binding agent until the molding batch looked uniform. The use of polyimide (Matrimid) and polysulfone polymers as matrices in synthetic polymer–MOF composite membranes has been investigated. The composite membranes of MOF-5 and ZIF-8 with Matrimid were fabricated [59, 60]. A solution of Matrimid in $CHCl_3$ was combined with a dispersion of presynthesized MOF-5 or ZIF-8. Sonication was employed to disperse the MOF crystals, followed by solvent evaporation to form the composite membrane. The composite membrane's plastic deformation indicated a strong interconnection between the MOF-5 nanocrystals and the polymer matrix. Composite membranes of HKUST-1, MIL-47, MIL-53, and ZIF-8 with Matrimid or polysulfone were also prepared using the same method [61, 62]. Additionally, ZIF-8–polysulfone membranes were fabricated using the solution blending technique, and incorporation of ZIF-8 crystals enhanced the gas permeation assets of the composite, particularly in terms of CO_2 diffusion [63].

Additionally, synthetic polymer fibers were employed as substrates to fabricate MOF composites. For instance, well-dispersed ZIF-8 nanocrystals were incorporated into a polyvinylpyrrolidone (PVP) solution to produce ZIF-8/PVP composite nanofibers [64]. Furthermore, the stability of the composite material could be optimized by utilizing alternative polymers such as polystyrene and polyethylene oxide. MOF/polymer composite fibers can also be synthesized with varying mechanical stabilities (MOF: HKUST-1, MIL-100; polymer: PS, PVP, polyacrylonitrile, and polypropylene) [65]. Lower MOF loadings and a pearl necklace-like morphology were the results of a little variation in particle size and fiber diameter. Thankfully, with greater MOF loadings, particles combined with noticeably smaller strands produced a spiderlike shape. Composites can also be created using fibers made of natural polymers. For example, pulps with varying treatments were used to prepare composite of HKUST-1 with uneven dispersion when added to the pulp slurry [66]. The direct growth method resulted in pulp fibers with uniformly distributed crystals across the surface area. This even distribution was ascribed to the presence of carboxyl groups in lignin. To enhance mechanical stability and facilitate handling compared to bulk HKUST-1, polyacrylamide (PAM) beads were employed as a matrix due to their hydrophilic nature, in combination with HKUST-1 and Co-CPO-27 [67]. Two distinct techniques were utilized in this process: the beads were dissolved in hot crystallization solutions and formed under solvothermal conditions. When the beads were preswelled in a 1:1 ethanol/water combination before solvothermal treatment, the crystals only grew on the outside, suggesting a high diffusion barrier in comparison to the rate of nucleation and crystal formation. By altering the HKUST-1 reaction mixture's concentration, the MOF:polymer ratio may be changed. HKUST-1 crystals were not formed by the immersion process of untreated beads. HKUST-1/PMA composites were therefore formed as a result of pretreatment, which involved preswelling the PAM beads in a copper acetate

solution. Solvothermally synthesized Co-CPO-27/PAM beads only displayed crystals on the exterior surface, regardless of the pretreatment. Composite SiO2/PAM beads were examined in addition to pure organic beads. HKUST-1 crystals were produced on SiO_2/PAM beads using the immersion technique.

Enzyme-MOF Composites

A very effective family of biocatalysts, with their high activity and chemo-, enantio-, and regioselectivity, enzymes can catalyze a variety of activities in moderate circumstances. But the delicate characteristics of enzymes, such as their low resistance to organic solvents and denaturants, limited optimal pH ranges, and low heat stability, significantly limit their extensive catalytic uses. Furthermore, the presence of enzyme contamination in the intended products necessitates laborious purifying and separation procedures. It has been demonstrated that MOFs are attractive platforms for immobilizing enzymes to protect them from deactivating reaction conditions, increase their recyclability, and reduce product impurity [68–70]. Because MOFs' pore size, shape, and structure can be precisely controlled, enzymes of a similar size may be contained, reducing leaching and enzyme self-aggregation [70]. To prevent enzyme leaching, the inorganic nodes and functional linkers of MOFs can interact with enzymes through coordination bonds, covalent bonding, hydrogen bonding, and van der Waals forces. Various strategies for enzyme immobilization within MOFs have been reported, including physical adsorption, diffusion, covalent bonding, and coprecipitation [70].

Weak interactions between the enzyme and MOF crystals, such as electrostatic interactions, hydrogen bonds, and van der Waals forces, are necessary for physical adsorption. While maintaining enzymatic structure and function, these weak interactions increase enzyme stability. Multiple covalent connections can be used to bind enzymes to MOF crystals, significantly improving long-term stability. Another successful tactic is the diffusion of enzymes into MOF pores, where mesoporous MOFs are employed to accomplish high enzyme loading and effective substrate diffusion [68].

By using a coprecipitation technique, enzymes may be encapsulated in situ during the MOF synthesis process rather than being added to the presynthesized MOF holes. ZIFs with moderate synthetic conditions can be used as a protective shell for this technique to prevent denaturation of the enzyme during the encapsulation process [71]. Furthermore, ZIFs' tiny holes will reduce the amount of enzyme that leaks out of them while still allowing substrates to pass through the framework and get to the enzymes that are encapsulated. Controlling enzyme localization, substrate and product diffusion, enzyme and coenzyme accessibility, and enzyme-support interactions are crucial factors that impact the catalytic efficiency of immobilized enzyme composites in enzyme immobilized systems. In this sense, the functionality and structure (pore connectivity and topology) of MOFs greatly influence how well enzymes work.

Proteins have a recognized tendency to be more attracted to hydrophobic surfaces, and these interactions frequently result in conformational changes that denature the protein and cause it to lose its function. To examine the activity of

encapsulated enzymes, urease and catalase were encapsulated within three Zn-based ZIFs with distinct hydrophobicity and hydrophilicity but similar structural metrics (Fig. 5a) [72]. The hydrophilic MAF-7 and ZIF-90 encased FCAT maintained its enzymatic activity in H_2O_2 decomposition. However, there was no detectable catalytic activity from FCAT enclosed in hydrophobic ZIF-8. The hydrophobic contacts between FCAT and ZIF-8 may cause FCAT to aggregate, which might impede the diffusion of the substrate (H_2O_2) and the product (H_2O), owing to ZIF-8 hydrophobic environment. This could be the cause of the decrease in FCAT activity in ZIF-8 [72].

Several enzymes, coenzymes, substrates, and products participate in chemical transformations in biological systems. The substrate and coenzymes must be let to diffuse and interact with the encapsulated enzymes in order to accomplish a complex biochemical transformation in MOF pores. As a result, it is critical to develop a MOF structure with an appropriate topology (pore/channel shape) for encapsulating enzymes and high interpore connection for enzyme accessibility. In three channel-

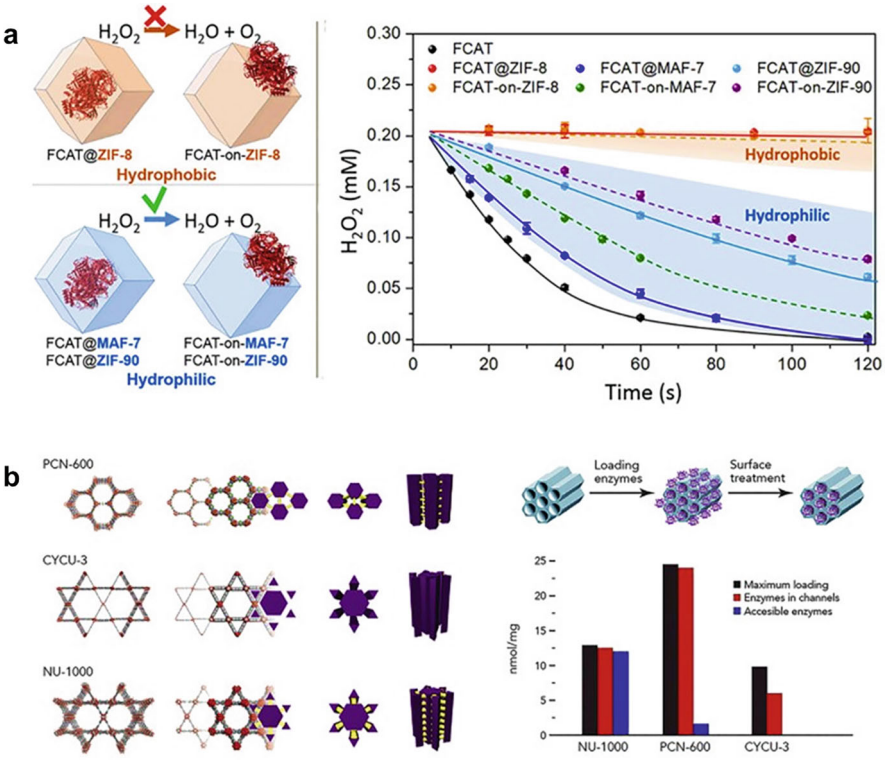

Fig. 5 (**a**) Hydrophilic MAF-7 and ZIF-90 encased FCAT maintained its enzymatic activity in H_2O_2 decomposition. (Reproduced from Ref. [72]). (**b**) Encapsulating enzymes and high interpore connection in three channel-type MOFs (NU-1000, PCN-600, and CYCU-3). (Reproduced from Ref. [73] © 2016 Elsevier)

type MOFs with comparable mesopore diameters (about 3.0 nm) but distinct channel systems and connectivity, Farha and colleagues studied the immobilization of an enzyme (such as cutinase) (Fig. 5b) [73]. The hierarchical pore structure of NU-1000, characterized by one-dimensional 3.1 nm hexagonal and 0.8 nm triangular channels interconnected by microporous windows, facilitates cutinase stability within the mesopores while allowing the free diffusion of reactants and products through the micropores. The microporous windows connecting the mesopores enhance this diffusion process. In contrast, PCN-600 contains only one-dimensional 3.0 nm hexagonal channels with windows linking them. Upon encapsulation of cutinase, these mesopores become obstructed, limiting the available volume for reactant diffusion. While CYCU-3 shares a similar hierarchical pore structure to NU-1000, it lacks interconnecting windows, hindering substrate diffusion across the triangular channels to access the enzyme within the mesopores.

A titration experiment utilizing an organophosphorus ester containing a fluorescent resorufin group as an active-site titrant demonstrated that cutinase was accessible within these MOFs. The titration results indicated that only 6% of the cutinase encapsulated in PCN-600 retained activity, whereas 93% of the cutinase encapsulated in NU-1000 remained accessible and catalytically active.

With its hierarchical pore structure and channel-connecting windows, NU-1000 demonstrated comparable overall activity to free cutinase in solution while hydrolyzing p-nitrophenyl butyrate.

To create a NU-100x series with hierarchical pore networks made up of hexagonal and triangular channels associated by diamond-shaped windows, pores of MOF were enlarged. These channels served as platforms for the immobilization of enzymes, such as lactate dehydrogenase (LDH) [74]. With more room for enzyme and coenzyme recognition, channel and bridging window enlargement may promote the diffusion of substrates and coenzymes. As the size of the supports' pores rose, so did the activity of the encapsulated LDH. With more room for enzyme and coenzyme recognition, channel and bridging window enlargement may promote the diffusion of substrates and coenzymes. As the size of the supports' pores rose, so did the activity of the encapsulated LDH. LDH immobilized in NU-1005 had an initial reaction rate that was almost the same as free LDH. They also constructed a typical catalytic system that included the coenzymes nicotinamide adenine dinucleotide (NAD and NADH), diaphorase, and LDH. While NU-100x's ($x = 3, 4$) triangular channels are too tiny to hold NAD+, NU-100x's ($x = 5, 6$, and 7) are large enough. Interestingly, the two latter MOFs had slower apparent response rates than free LDH, but the three former MOFs achieved reaction rates that were 1.5–3 times higher than free LDH. This study shows that the accessibility of the encapsulated enzymes and the diffusion rates of the substrate and coenzymes are influenced by the size of the MOF pores. Given that charged MOFs may exhibit electrostatic affinity with oppositely charged substrates, the electrostatics of MOFs may also influence the performance of enzyme@MOF composites. As a durable and reusable biocatalyst for the oxidation reaction of dyes, Ricoux and colleagues employed MIL-101(Cr) to encapsulate a peroxidase-type enzyme (microperoxidase-8 MP8). MIL-101 might pre-concentrate the substrate for a faster reaction rate in the

enzymatic catalytic reaction in addition to serving as a stabilizing host to improve the stability and reusability of the encapsulated enzyme.

MIL-101(Cr), with a positive charge in the pH range of 5–7, demonstrates a preferential affinity for the negatively charged methyl orange (MO) over the positively charged methylene blue (MB). Catalytic data revealed that MP8@MIL-101 (Cr) oxidized the negatively charged dye (MO) at higher reaction rates compared to free MP8. Consequently, the electrostatically favorable interactions between MO and the MOF matrix likely enhance the diffusion of MO into the MOF pores, promoting the pre-concentration of MO around the enzyme and consequently improving its catalytic activity.

Polymer-MOF Composites

MOFs have been shown by several studies to be possible reinforcements in polymer matrices that can enhance a variety of characteristics and provide the producing material intriguing new capabilities. The covalent attachment of MOFs to the surface of polymers is a common approach for synthesizing MOF/polymer composite materials, with grafting achievable through various techniques. Liang et al. [75] demonstrated that the polymer composite incorporating MOFs exhibited superior low-humidity proton conductivity compared to the chiral two-dimensional MOF. The produced MOF's structural characteristics aided in the conduction of protons. The MOF submicrorods are evenly dispersed and blended throughout the polyvinylpyrrolidone matrix.

Physical characteristics like solubility and moisture absorption are diminished by the increased porosity, although they can be enhanced by combining MOFs with functional polymers. To improve MOF's interfacial interactions with polymer matrices, the aforementioned polymers can serve as a bridge. Nonetheless, the addition of MOF to polymers mostly improves their ability to suppress corrosion and to withstand flames.

MOF-polymer composite materials, including MOF-supported membranes and MOF-based mixed-matrix membranes (MMMs), have garnered significant attention in recent research. There are three primary strategies for the emulsion templating synthesis of MOF-polymer composites: (1) growing MOF crystals on an already synthesized polymer support, (2) performing polymerization around preformed MOF crystals, or (3) copolymerizing monomers with MOFs that have been modified with polymerizable functional groups. Abbasi et al. [76] investigated a simple phase inversion method for fabricating ZIF-8/polymer composite beads, demonstrating their effectiveness in oil sorption applications. The study revealed that ZIF-8 particles were uniformly coated and distributed across the surface of the polymer bead composites at higher loadings, optimizing oil sorption.

MOF–polymer composites have recently been produced using one-step synthesis techniques based on the emulsion templating method and polymerization of the emulsion's internal phase. For the creation of porous MOF-polyHIPE composites, this emulsion templating technique has concurrently caused crystallization and polymerization in the emulsion's internal phase. One-step synthesis of MOF-polyHIPE composite materials may result in a discernible increase in mechanical stability, which might expand their potential uses across a range of industries [77].

Even though conjugated polymers have amazing properties, there are certain restrictions on how they may be used. Making composites of CPs with mechanically strong materials, such as MOFs, is a clever way to lessen the disadvantages of CPs and improve their significant intrinsic qualities. Because of their remarkable porosity, huge SSA, and remarkable mechanical and thermal durability, MOFs may readily address the drawbacks of CPs [78]. Because of the ideal combination of CPs and MOFs, their composites perform better and are thus widely used in several applications. For instance, Milakin et al. used an in situ polymerization technique to create a binary PANI/Fe-BTC composite. They studied the effects of changing the ratio of monomers in the original polymerization mixture on the performance and structural properties of the resulting composite materials [79]. Similarly, in recent years, a lot of study has been done on the hybridization of PPy (polypyrrole) with different MOFs. Functional materials appropriate for use as supercapacitor electrodes have been produced using this combination. These composite materials have demonstrated very promising properties by utilizing their large surface area and superior electrical conductivity.

Most MOF/polymer composites are fabricated using a post-synthesis approach, which can be categorized as either "grafting to" or "grafting from," depending on the initiation site of the polymerization. The interactions between the MOF and polymer can be either covalent or non-covalent, depending on the functional groups present on both components. An example of such a composite is UiO-66-NH_2@PMAA, developed by Lie et al. in 2017, using a combination of click chemistry, post-synthetic modification (PSM), and atom transfer radical polymerization (ATRP). They selected polymethacrylic acid (PMAA) to coat the MOF due to its abundant functional groups, such as carboxylic acids for electrostatic interactions with the $-NH_2$ groups of enzymes and alkynyl moieties capable of reacting with the amine groups of UiO-66-NH_2. Additionally, MOFs can be encapsulated and protected with porous organic polymers (POPs), which provide photoactive molecular blocks for biomedical applications. When there is strong interaction between the MOF and POP, a core-shell nanocomposite can be synthesized, with the MOF acting as a template for POP formation. However, the large size of the resulting composite and its poor dispersibility in aqueous solvents limit its practical applications.

Inorganic Matrix-MOF Composites

For the creation of composites, four distinct kinds of inorganic matrices graphite oxide (GO), silica, alumina, and cordierite, or mixtures of these were used.

The covering of a cordierite monolith was the subject of two research. The secondary growth approach was used to achieve uniform coatings of Cr-MIL-101 nanocrystals inside the macropores of a cylindrical cordierite monolithic [80]. Two techniques were used: (a) the substrate was dip-coated with an α-alumina suspension before being seeded with premade Cr-MIL-101 nanocrystals, and (b) the substrate was dip-coated with an α-alumina suspension and preformed Cr-MIL-101 nanocrystals. When reaction conditions were optimized, such as when the autoclave

rotated during the secondary growth stage and the seed size was appropriately chosen, a dense, homogeneous coating was seen.

Graphite oxide (GO) was dispersed in the synthesis mixtures before the solvothermal processes to create composites of MOF-5 [81] and HKUST-1 [82], which improved GO's gas adsorption capabilities. GO/MOF-5 composites were produced with different component ratios. Microporosity was found to decrease with increasing GO concentration. Due to potential interactions between the oxide clusters in MOF-5 and the epoxy groups on graphene, the composites most likely adopted lamellar structures made from alternating layers of GO and MOF. Additionally, GO/HKUST-1 composites were reported, with the composite's porosity allegedly surpassing that of the parent materials. Regretfully, the authors reported a less specific surface of for their material, which is significantly less than state of art values.

The production of GO/Fe-MIL-100 composites has also been studied recently. Higher GO concentrations in these investigations were associated with increasing quantities of an amorphous phase [83]. The creation of hierarchical micro- and mesoporous HKUST-1/alumina and HKUST-1/silica composites was examined using a nonionic surfactant. These were made by subjecting a dispersion of HKUST-1 starting materials, an alumina (boehmite) or silica (TEOS) source, and the triblock copolymer Pluronic P123 to MW irradiation [84]. Sorption studies were able to demonstrate both microporosity and mesoporosity for the composites, while XRPD measurements verified the presence of HKUST-1.

For the manufacture of HKUST-1 composites, silica and alumina beads were also used as substrates. After impregnating monodisperse mesoporous silica beads (Nucleosil 100-3) with the initial mixture, the solvent was removed [85]. The monodisperse MOF–silica composites showed good separation capabilities when evaluated as the HPLC stationary phase [67]. Silica and SiO_2/Al_2O_3 composite beads were employed in another report. Two techniques were used: the beads were dissolved in hot crystallization solutions and formed under solvothermal conditions. On silica beads, no HKUST-1 growth was seen; however, on mixed SiO_2/Al_2O_3 beads, growth was noted. This was ascribed to the alumina's more fundamental characteristics. There was no information provided about the development of the beads' macropores or their surface.

Metal Nanoparticles/Cluster-MOF Composites

When combined with MOFs, metal nanoparticles (NPs) are the most often investigated particles among the many functionalized materials, improving the nanocomposite's characteristics and potential uses [86]. The well-defined porosity and crystalline character of MOFs, which allow NP dispersion rather than aggregation, may be the reason why MOFs are known to stabilize the structures of metal and metal oxide NPs. The three primary synthetic techniques for stabilizing NPs in the presence of MOFs are (i) direct mixing of NP and MOF precursor solutions, which results in the formation of nanocomposite structures and spatial growth; (ii) assembling NPs precursors into MOF cavities and further reaction conditions that produce the functional structure of the nanocomposite; and (iii) epitaxial growth

of MOFs onto NPs, in which the synthesized NPs are treated to MOFs precursor solution, which causes the grown MOFs surrounding the NPs to stabilize the NPs [87]. Functional groups, organic linkers, the size difference between NPs and MOFs, and the reaction solvent all appear to be important factors in stabilizing NPs and promoting MOF hetero-nucleation onto NP surfaces in all of these techniques. The active sites of NPs are occasionally blocked by the surfactants employed to create the MOFs nanocomposite and surfactant-encapsulated NPs.

Through capillary force and hydrophilic contact, NPs with a volume slightly less than the MOF pore volume throughout the reaction likely to be adsorbed into the pores of dehydrated MOFs. Additionally, 20% H_2/Ar is added to the resultant MOF composites to decrease them and create Pt and Pt/Cu NP encased MIL-101 nanocomposite structures. Studies also demonstrate the creation of nanocomposite materials, in which MOFs constitute the shell coat and NPs form the core, in addition to NPs being assembled into the pore cavities of MOFs. In order to cover the surface of Pd nanocrystals with MOF (HKUST-1) [86] created a nanocomposite material.

Pd nanocubes were first created for the investigation by reducing Na2PdCl4 with ascorbic acid and then covering it with bromide ions. After that, HKUST-1 was applied by suspending Pd nanocubes in an ethanolic solution that contained trimesic acid and $Cu(NO_3)_2{\cdot}3H_2O$. The production of MOF nanocomposite materials has been reported to employ a variety of different NPs, including Au, Ag, Cu, Mg, Ni, Pt, and Ru, in either monometallic or bimetallic forms.

Using the double-solvent technique (DSA), $Pd(NO_3)_2$ was introduced into the MOF pores to create the Pd NPs in UiO-66-X, resulting in Pd@UiO-66-X with comparable Pd loadings (0.9–1.1 wt%). Additionally, Pd/UiO-66 was made as a control in order to guarantee that all Pd NPs are on the MOF's exterior surface (Fig. 6a). To be precise, the premade Pd_{PVP} nanoparticles (NPs) measuring around 3.5 nm were coated with poly(vinylpyrrolidone) (PVP) and joined with UiO-66 via electrostatic contact. PVP was then removed to produce Pd/UiO-66 with a Pd loading of 0.94 weight percent [88].

Instead of surface decoration, metal nanoparticles have also been encapsulated as core matrix in the pores of MOFs. For example, PVP capped Pt NPs (Pt_{PVP}), Pt with partially removed PVP (Pt_{rPVP}), and clean Pt without PVP (Pt) are incorporated in MOF as a photosensitizer and support. These nanocomposites have comparable particle sizes (approximately 2.5 nm) and loadings (approximately 2.5 wt%), resulting in Pt_{PVP}@UiO-66-NH_2, Pt_{rPVP}@UiO-66-NH_2, and Pt@UiO-66-NH_2 (Fig. 6b) [89]. Surprisingly, the progressive elimination of interfacial PVP promotes electron transport between the MOF and Pt sites and increases electrical conductivity. Pt@UiO-66-NH_2 significantly inhibits electron-hole recombination, which results in its significantly higher activity [90].

Chen et al. [91] used a twofold solvent approach technique to insert mono- and bimetallic NPs into MOF structures. For this, the MOF was $Cr_3X(H_2O)_2O(BDC)_3{\cdot}nH_2O$ (BDC = benzene-1,4-dicarboxylate, X = F or OH, n = ~25), and the NPs precursor solution was $H_2PtCl_6{\cdot}6H_2O$ and $Cu(NO_3)_2{\cdot}3H_2O$. Mesoporous MOF (Cr-MIL-101), which has a large specific surface area of >3600 $m^2\ g^{-1}$ (BET), appropriate pores (2.9 and 3.4 nm), and two pore windows of approximately 1.2 and

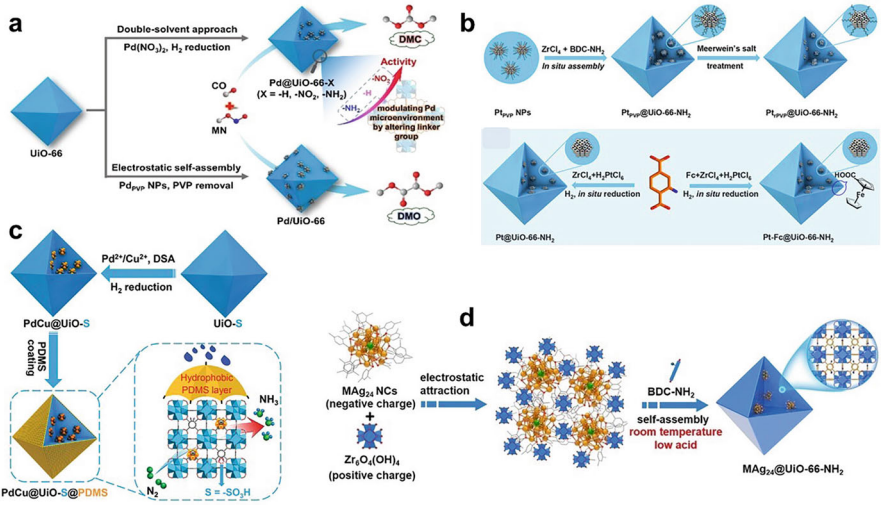

Fig. 6 Schematic illustrations for the synthesis of nanoparticles@MOF. (**a**) Preparation of Pd/UiO-66. (Reproduced from Ref. [88]). (**b**) Pt@UiO-66-NH_2. (Reproduced from Ref. [89]). (**c**) Bimetallic nanoparticles (PdCu@UiO-S). (Reproduced from Ref. [92]). (**d**) Bimetallic nanoclusters ($AuAg_{25}$@UiO-66-NH_2). (Reproduced from [93] copyright © 2024 Wiley-VCH GmbH)

1.6 nm, respectively, encapsulated platinum (Pt) and copper (Cu) nanoparticles (NPs) with diameters of 1.5 and 1.7 nm.

When heated, the UiO-66-SO_3H (UiO-S) may be activated to add metal nanoparticles and twofold solvent approach synthesis procedure was used to insert Pd and PdCu NPs to produce Pd@UiO-S and PdCu@UiO-S, respectively (Fig. 6c). In order to stop the development of metal NPs on the MOF external surface and prevent their aggregation, the MOF's hydrophilic cages allow for the entire introduction of the metal precursor aqueous solution by capillary force and hydrophilic contact. This metal precursor was then further reduced by H_2 to produce metal NPs that were contained within the MOF [92].

Despite the single metal nanoparticles at the core, the multi-metals have a classic impact on the performance of composites. For instance, four MAg_{24} (M = Ag, Pd, Pt, and Au) nanoclusters (NCs) have been electrostatically encapsulated into a typical visible-light-responsive MOF, UiO-66-NH_2 (Fig. 6d). $AuAg_{25}$@UiO-66-NH_2 remarkably exhibited exceptional activity and retained good stability in the photocatalytic hydrogen generation process [93]. One efficient way to improve the selectivity and activity of catalytic processes is to modify the chemical microenvironment of NPs. In order to systematically investigate the impact of the hydrophobic microenvironment on the electrocatalytic activity, a post-synthetic modification strategy was developed to modulate the hydrophobic microenvironment of Ru nanoparticles encapsulated in MOF. The competitive hydrogen evolution process (HER) can be successfully suppressed by increasing the catalyst's hydrophobicity over time by the lengthening of the perfluoroalkyl chain [94].

Metal Oxide-MOF Composites

Metal oxides, metal nitrides, and some transition-metal macrocycles are also employed as electrocatalysts, much like metal particles. Because of their superior ORR catalytic activity, cheap cost, and environmental compatibility, manganese oxides are seen as prospective substitutes for Pt-based catalysts [95]. Although MnO_2 has been utilized extensively as an ORR catalyst in recent years, the agglomeration of particles during the reaction limits its ORR catalytic activity. To efficiently avoid agglomeration, ε-MnO_2 produces nanorods when it is placed into the FeBTC framework. One end of the nanorods protrudes, while the other end is securely fixed onto the FeBTC framework.

As a result, the composite exhibits better ORR activity in alkaline solution than ε-MnO_2 and MOF(Fe) + ε-MnO_2, which is comparable to 20% Pt/C. When O_2 is first reduced to H_2O_2 and then chemically decomposes to create OH^- and O_2, a clear four-electron transfer takes place during the ORR process of the ε-MnO_2@FeBTC composite. The FeBTC MOF with micropores has a large specific surface area, which facilitates oxygen transport and enhances ORR catalytic activity.Due to its optical, electrical, and chemical stability, SnO_2 has garnered a lot of interest as an electrode material for supercapacitors. Because of their electric double layer capacitance, SnO_2 quantum dots in particular show highly noticeable oxidation–reduction peaks, indicating the presence of Faradaic processes.

ZIF-8 is a typical MOF that shows ultrastability even in boiling alkaline water and organic solvents. Using a straightforward in situ epoxide precipitation technique, Tang and colleagues have distributed SnO_2 quantum dots into a ZIF-8 framework to create SnO_2 quantum dots@ZIF-8 composite [96]. The electrochemical measurements indicate that the SnO_2 quantum dots@ZIF-8 material performs very well, exhibiting a high capacitance of 931 F g^{-1} at 5 mV s^{-1} in an electrolyte of 6 m KOH. Compared to ZIF-8 (99 F g^{-1}) and SnO_2 quantum dots (241 F g^{-1}), this result is significantly greater. SnO_2 quantum dots and ZIF-8 with a porous structure work together to optimize the use of active material. Over 500 cycles, this composite exhibits good cycling stability.

Additionally, using ZIF-8 as the host, a new Cu_xO nanoparticle@zeolitic imidazolate framework (Cu_xO NP@ZIF-8) was created [97]. Because ZIF-8 can maintain its original structure at the same pyrolysis temperature, their synthesis is intriguing. This composite Cu_xO NP@ZIF-8 is the result of the simple pyrolysis of HKUST-1@ZIF-8 nanocrystal based on the different thermal stability of the two MOFs, where HKUST-1 is transformed into Cu_xO NPs that uniformly disperse inside the host materials of ZIF-8. This material functions as an electrochemical sensor that detects H_2O_2 with a high sensitivity of 0.15 × 10^{-6} m and a broad detection range of 1.5–21,442 × 10^{-6} m. This kind of performance results from the combined action of effective Cu_xO NP electrocatalysis and the right pore size and shape for ZIF-8.

The ZnO@ZIF-8 composite may be prepared for electrochemical response by embedding semiconductive ZnO nanoparticles into the ZIF-8 cavities. Zhan et al. created a straightforward self-template technique for creating metal oxide

semiconductor@MOF core–shell heterostructures using vertically standing arrays and freestanding ZnO@ZIF-8 nanorods. ZnO nanorods serve as the Zn^{2+} supply and template for ZIF-8 growth during the production. When serous buffer solution is present, the as-synthesized ZnO@ZIF-8 nanorod arrays clearly show a photoelectrochemical sensing response to H_2O_2. Furthermore, the molecule-size-selective ability of the MOF shell is responsible for the interesting catalytic capabilities of such a MOF composite with multifunctional core–shell heterostructures in electrochemical catalysis [98].

Carbon-MOF Composites

Nitrogen-doped carbon graphite (g-C_3N_4), graphene, graphene oxide (GO), reduced graphene oxide (rGO), carbon nanotubes, and fullerenes are examples of carbon-based materials that are frequently utilized as substrates to produce materials with favorable electrical characteristics.

These carbon materials (such as carbon fiber, graphene, carbon nanotubes, and XC-72) are distinguished by their high specific surface area, varied functional groups, and strong conductivity. Composites made of MOF and carbon materials are used extensively in electrochemical sensing because of their high porosity, large specific surface area, high catalytic efficiency (attributed to MOF), and strong conductivity (attributed to carbon materials).

Single- or multilayer graphite sheets that have been hybridized with sp^2 carbons and wound around the central axis at a certain helix angle form the seamless cylindrical tubes known as carbon nanotubes (CNTs). Multi-walled carbon nanotubes (MWCNTs) and SWCNTs are two examples; they are distinguished by their high conductivity, huge specific surface area, and good chemical stability. Composites including MOF and CNTs have therefore been employed to create electrochemical sensors with great selectivity and sensitivity [99]. Using a solvothermal technique, Rani et al. [100] created the Sn-MOF@CNT composite. While CNTs can offer quick electron transport pathways, the built Sn-MOF has a large specific surface area and a porous structure. For the electrochemical detection of H_2O_2, electrochemical sensors with Au electrodes modified by the Sn-MOF@CNT composite performed exceptionally well.

MOF-MOF or MOF-COF Composites

MOFs may directly incorporate multifunctional predesigned active sites and improve the capacity of photogenerated electron-hole pairs to separate when paired with other reticular frameworks, such as MOFs or covalent frameworks (COFs) [101, 102]. By integrating MOFs with reticular frameworks that exhibit semiconductor characteristics, the system's light sensitivity may be increased, allowing for light stimulation. Since Kitagawa and his colleagues used the epitaxial growth method to create MOF-MOF composites [103], an increasing number of MOF-MOF composite structures (yolk-shell [104], core-satellite [105], and asymmetric structures [106]) have been created for various uses.

Using a straightforward one-pot technique, Cao and his colleagues created a core-shell heterojunction of PCN-222-Ni@UiO-67-NH_2 (P@U) [107]. Following

illumination, UiO-67-NH_2 generates electrons, which are then quickly transported to PCN-222-Ni. Without the need for further sacrificial agents, photocatalytic CO_2RR was able to create formic acid at a record level (146.0 μmol g^{-1} h^{-1}) thanks to the resultant material's wide range of light response and optimal substrate enrichment. Through surface ligand exchange from 2-methylimidazole to 2,5-dihydroxyterephthalate, which creates strong coordination bonding, ZIF-67 was transformed into ZIF-67@Co-MOF-74. The shell thickness was regulated by altering the quantity of second ligand. The catalytic capabilities of pure ZIF-67 and Co-MOF-74 were then assessed and contrasted with those of the ZIF-67@Co-MOF-74 series with varying thicknesses. As their shell thickness rose, the core-shell MOFs improved photocatalytic performance [108].

In order to overcome the limitations of lattice matching rule, internal extended growth method (IEGM) was introduced for designing/synthesizing modular hierarchically MOF composites. By using microwave heating, NH_2-UiO-66(Zr) was exposed to precursors of NH_2-MIL-125(Ti) with PVP as the structure-director agent; two MOFs with different morphologies and crystal structures were readily hybridized as MOF-on-MOF heterostructures [105].

Over the past 20 years, a lot of research has been done on the development and design of multi-metal MOF crystals. Nevertheless, a MOF-on-MOF material that is better than a single crystal is created when several MOF crystals nucleate and develop on the original MOF. When compared to well-developed single MOFs, MOF-on-MOF composites, which are created by combining two or more MOFs, often show more structural variety and more possibilities. In this regard, it is extremely difficult to build MOF-on-MOF heterostructures in an orderly manner with precisely defined compositions, morphologies, and interfaces for particular functions that exhibit better performance in a variety of applications.

The successful creation of MOF-MOF composites has led to the progressive application of COFs, or reticular frameworks made of covalent bonds, to related structures. Zhang and his colleagues created NH_2-MIL-68@TPA-COF by using amino groups in rod-like NH_2-MIL-68 as the base and growing sheet-like TPA-COF as its outer layer via Schiff base condensation [109]. This was the first report of COF-MOF composites and was able to efficiently photodegrade Rhodamine B. Later, the condensation reaction between -NH_2 and -CHO was used to create this kind of composite, and it became a popular tactic [110].

From a structural perspective, the energy band structures of the catalysts may be considerably controlled by adding COF materials, which typically have a large conjugated structure. To further achieve the objective of photocatalytic overall reactions, the C=N bond with dynamic covalent bond properties can facilitate the spatial separation of photogenerated charges and holes, and the catalyst design can clearly spatially separate the oxidation site from the reduction site [111]. The MOF-in-COF membrane idea was recently introduced and ZIF-67 was restricted to grow inside the pores of TpPa-1 membrane. The resultant ZIF-67-in-TpPa-1 membrane had exceptional separation performance, which was attributed to the unique MOF-in-COF micro/nanopore network [112]. Similarly, Gao et al. created ZIF-67-in-PBD membranes for H_2/CH_4 separation [113]. Since it is challenging to control MOF

formation within the COF pores, the growth of MOF in COF pores is currently accomplished via a prolonged immersion fueled by a weak capillary force. Furthermore, MOF may develop on the surface of the COF membrane rather than in its interior pores if the membrane is submerged in the reaction solution for an extended period of time. To overcome this drawback, a vacuum-assisted perfusion method was developed to produce ZIF-8@TB-COF composite membrane. The pore diameter of TB-COF is approximately 2.7 nm, whereas ZIF-8's unit cell size is around 1.7 nm. Consequently, ZIF-8 unit cells may be accommodated in the TB-COF pores to create distinct hierarchical micro/nanochannels for gas permeation [114].

Conclusion

The structure-performance of MOF-based composites was outlined, emphasizing the roles of MOF moieties in real-world applications. When compared to single-component materials, MOF composites using MOFs invariably shown noticeably improved or even unique characteristics. MOFs can be used in practical applications as active site supports, separation membranes, electronic structure modulators, catalytic site stabilizer, etc. There are several techniques have been developed to synthesize MOF composites by tuning the structural and electronic properties of MOFs and combining materials. It is proven by the previously studies on MOF-based composites that these materials' structures and characteristics may be altered to suit the needs of the applications. The characteristics of MOFs can be significantly improved by adding functional nanomaterials to create MOF composites. Functional materials can serve as scaffolding to restrict MOF particles, which might make it easier to process and formulate MOF composites into configuration-tailored materials for particular applications. Synergistic effects between the components are demonstrated by MOF composites, which have outstanding properties that significantly increase a wide range of the applications.

Cross-References

- ► Application of Metal-Organic Frameworks in Analytical Chemistry
- ► Cage-Like Metal-Organic Frameworks Based on Carboxylate Ligands
- ► Crystal Topology for the Study and Design of Metal-Organic and Covalent-Organic Frameworks
- ► Design and Synthesis of Metal-Organic Frameworks
- ► Historical Development of Metal-Organic Frameworks

Competing Interest Declaration The author(s) has no competing interests to declare that are relevant to the content of this manuscript.

References

1. Cai X et al (2020) Nano-sized metal-organic frameworks: synthesis and applications. Coord Chem Rev 417:213366
2. Ding M et al (2019) Carbon capture and conversion using metal–organic frameworks and MOF-based materials. Chem Soc Rev 48(10):2783–2828
3. Li D et al (2024) Advances and applications of metal-organic frameworks (MOFs) in emerging technologies: a comprehensive review. Global Chall 8(2):2300244
4. Ding M, Jiang H-L (2021) Improving water stability of metal–organic frameworks by a general surface hydrophobic polymerization. CCS Chem 3(8):2740–2748
5. Moosavi SM et al (2018) Improving the mechanical stability of metal–organic frameworks using chemical caryatids. ACS Central Sci 4(7):832–839
6. Meekel EG et al (2024) Enhanced elastic stability of a topologically disordered crystalline metal–organic framework. Nat Mater 23(9):1245–1251
7. Hou X et al (2022) Strategies for induced defects in metal–organic frameworks for enhancing adsorption and catalytic performance. Dalton Trans 51(21):8133–8159
8. Liu J et al (2022) Post-synthetic modifications of metal–organic cages. Nat Rev Chem 6(5): 339–356
9. Sun N et al (2025) MOF-based electrocatalysts: an overview from the perspective of structural design. Chem Rev 125(5):2703–2792
10. Chen L et al (2020) The function of metal–organic frameworks in the application of MOF-based composites. Nanoscale Adv 2(7):2628–2647
11. Pastore VJ, Cook TR, Rzayev J (2018) Polymer–MOF hybrid composites with high porosity and stability through surface-selective ligand exchange. Chem Mater 30(23):8639–8649
12. Xie LS, Skorupskii G, Dincă M (2020) Electrically conductive metal–organic frameworks. Chem Rev 120(16):8536–8580
13. Verma P et al (2024) Expanding the design space of polymer–metal organic framework (MOF) gels by understanding polymer–MOF interactions. Chem Mater 36(19):9356–9369
14. Li C et al (2021) Recent development and applications of electrical conductive MOFs. Nanoscale 13(2):485–509
15. Zaman N, Iqbal N, Noor T (2025) An efficient, ecofriendly bimetallic Fe-In MOF and its g-C_3N_4 based composites for methanol oxidation reaction. J Inorg Organomet Polym Mater 35 (1):300–316
16. Li C et al (2025) Enhanced solar photocatalytic performance of the in-situ coupling g-C_3N_4 with Zn-Mof via promoting the generation of H_2O_2. Available at SSRN 5137869
17. Zhu H et al (2025) Cyclically generated phase segregation synergizing with Si enhances lithium-ion storage capability. ChemPhysChem 26(8):e202401007
18. Shah SSA et al (2021) Metal–organic framework-based electrocatalysts for CO_2 reduction. Small Struct 3(5):2100090
19. Pan M et al (2023) Review: synthesis of metal organic framework-based composites for application as immunosensors in food safety. Anal Chim Acta 1266:341331
20. Feng K et al (2021) A label-free electrochemical immunosensor for rapid detection of salmonella in milk by using CoFe-MOFs-graphene modified electrode. Food Control 130: 108357
21. Huang N et al (2018) Tailor-made pyrazolide-based metal–organic frameworks for selective catalysis. J Am Chem Soc 140(20):6383–6390
22. Wu L-Y et al (2019) Encapsulating perovskite quantum dots in iron-based metal–organic frameworks (MOFs) for efficient photocatalytic CO_2 reduction. Angew Chem Int Ed 58(28): 9491–9495
23. Ravipati M, Durai L, Badhulika S (2023) Single-pot solvothermal synthesis of single-crystalline nickel–metal organic framework nanosheets for direct iron fuel cell applications. ACS Appl Energy Mater 6(13):6901–6909

24. An H et al (2023) High-performance solar-driven water harvesting from air with a cheap and scalable hygroscopic salt modified metal–organic framework. Chem Eng J 461:141955
25. Zhu J et al (2018) Titanium-based metal–organic frameworks for photocatalytic applications. Coord Chem Rev 359:80–101
26. Yu D et al (2019) Enhanced photocatalytic ozonation of organic pollutants using an iron-based metal-organic framework. Appl Catal B Environ 251:66–75
27. Du Q et al (2020) Selective photodegradation of tetracycline by molecularly imprinted ZnO@NH2-UiO-66 composites. Chem Eng J 390:124614
28. Guo F et al (2019) Size engineering of metal–organic framework MIL-101(Cr)–Ag hybrids for photocatalytic CO_2 reduction. ACS Catal 9(9):8464–8470
29. Hu Z et al (2020) Modulated hydrothermal synthesis of highly stable MOF-808(Hf) for methane storage. ACS Sustain Chem Eng 8(46):17042–17053
30. Wang M et al (2018) Metal–organic frameworks (ZIF-67) as efficient cocatalysts for photocatalytic reduction of CO_2: the role of the morphology effect. J Mater Chem A 6(11):4768–4775
31. Liu J et al (2020) A metal–organic-framework-derived (Zn0.95Cu0.05)0.6Cd0.4S solid solution as efficient photocatalyst for hydrogen evolution reaction. ACS Appl Mater Interfaces 12 (9):10261–10267
32. Chen S et al (2020) Single-atom Ru-implanted metal–organic framework/MnO_2 for the highly selective oxidation of NO_x by plasma activation. ACS Catal 10(17):10185–10196
33. Choi KM et al (2017) Plasmon-enhanced photocatalytic CO_2 conversion within metal–organic frameworks under visible light. J Am Chem Soc 139(1):356–362
34. Jiang ZW et al (2020) Controllable synthesis of porphyrin-based 2D lanthanide metal–organic frameworks with thickness- and metal-node-dependent photocatalytic performance. Angew Chem Int Ed 59(8):3300–3306
35. Nasiri A et al (2019) A microwave assisted method to synthesize nano$CoFe_2O_4$@methyl cellulose as a novel metal-organic framework for antibiotic degradation. MethodsX 6:1557–1563
36. Crake A et al (2019) The effect of materials architecture in TiO_2/MOF composites on CO_2 photoreduction and charge transfer. Small 15(11):1805473
37. Xu C et al (2019) Turning on visible-light photocatalytic C−H oxidation over metal–organic frameworks by introducing metal-to-cluster charge transfer. J Am Chem Soc 141(48):19110–19117
38. Singh M et al (2020) Sonication enhances the stability of MnO_2 nanoparticles on silk film template for enzyme mimic application. Ultrason Sonochem 64:105011
39. Abazari R, Mahjoub AR, Salehi G (2019) Preparation of amine functionalized g-C_3N_4@H/SMOF NCs with visible light photocatalytic characteristic for 4-nitrophenol degradation from aqueous solution. J Hazard Mater 365:921–931
40. Hlophe PV, Dlamini LN (2019) Synthesis of a semi-conductor-like MOF with black phosphorous as a composite for visible light-driven photocatalysis. RSC Adv 9(64):37321–37330
41. Han B et al (2018) Nickel metal–organic framework monolayers for photoreduction of diluted CO_2: metal-node-dependent activity and selectivity. Angew Chem Int Ed 57(51):16811–16815
42. Zhao X et al (2017) A metal-organic framework approach toward highly nitrogen-doped graphitic carbon as a metal-free photocatalyst for hydrogen evolution. Small 13(9):1603279
43. Hayat A et al (2024) Recent advance in MOFs and MOF-based composites: synthesis, properties, and applications. Mater Today Energy 41:101542
44. Feng L et al (2020) An encapsulation-rearrangement strategy to integrate superhydrophobicity into mesoporous metal-organic frameworks. Matter 2(4):988–999
45. Li R et al (2023) Boosting the photocatalytic hydrogen evolution and NO removal via synergistic effects of in-situ Pt NPs formation and titanium integration in Zr-porphyrin MOFs. Fuel 336:126766

46. Ding D et al (2019) Impregnation of semiconductor CdS NPs in MOFs cavities via double solvent method for effective photocatalytic CO_2 conversion. J Catal 375:21–31
47. Hu M et al (2018) MOF-confined Sub-2 nm atomically ordered intermetallic PdZn nanoparticles as high-performance catalysts for selective hydrogenation of acetylene. Adv Mater 30 (33):1801878
48. Li M et al (2018) Synthesis of a 2D phosphorus material in a MOF-based 2D nano-reactor. Chem Sci 9(27):5912–5918
49. Gu Z-G et al (2017) MOF-templated synthesis of ultrasmall photoluminescent carbon-nanodot arrays for optical applications. Angew Chem Int Ed 56(24):6853–6858
50. Feng R et al (2022) In-situ cation exchange enhances room temperature phosphorescence of a family of metal-organic frameworks. SCIENCE CHINA Chem 65(1):128–134
51. Zhan W-W et al (2013) Semiconductor@metal–organic framework core–shell heterostructures: a case of ZnO@ZIF-8 nanorods with selective photoelectrochemical response. J Am Chem Soc 135(5):1926–1933
52. Zhan W et al (2016) Probing the structural flexibility of MOFs by constructing metal oxide@MOF-based heterostructures for size-selective photoelectrochemical response. Nanoscale 8(27):13181–13185
53. Li N et al (2021) NiO nanoparticles decorated hexagonal nickel-based metal-organic framework: self-template synthesis and its application in electrochemical energy storage. J Colloid Interface Sci 581:709–718
54. Stock N, Biswas S (2012) Synthesis of metal-organic frameworks (MOFs): routes to various MOF topologies, morphologies, and composites. Chem Rev 112(2):933–969
55. Wang W et al (2024) Metal-organic-framework-based materials as platforms for energy applications. Chem 10(1):86–133
56. Shi Y et al (2025) Prussian blue analogues "dressed" in MXene nanosheets tightly for high performance lithium-ion batteries. Adv Mater 37(8):2416665
57. Zhang G et al (2024) Dynamic phase transformations of prussian blue analogue crystals in hydrotherms. J Am Chem Soc 146(24):16659–16669
58. Schwab MG et al (2008) MOF@PolyHIPEs. Adv Eng Mater 10(12):1151–1155
59. Perez EV et al (2009) Mixed-matrix membranes containing MOF-5 for gas separations. J Membr Sci 328(1):165–173
60. Ordoñez MJC et al (2010) Molecular sieving realized with ZIF-8/Matrimid® mixed-matrix membranes. J Membr Sci 361(1):28–37
61. Basu S, Cano-Odena A, Vankelecom IFJ (2010) Asymmetric Matrimid®/[Cu3(BTC)2] mixed-matrix membranes for gas separations. J Membr Sci 362(1):478–487
62. Basu S et al (2009) Solvent resistant nanofiltration (SRNF) membranes based on metal-organic frameworks. J Membr Sci 344(1):190–198
63. Díaz K et al (2010) CO_2 transport in Polysulfone membranes containing Zeolitic Imidazolate frameworks as determined by permeation and PFG NMR techniques. Macromolecules 43(1): 316–325
64. Ostermann R et al (2011) Metal–organic framework nanofibers viaelectrospinning. Chem Commun 47(1):442–444
65. Rose M et al (2011) MOF processing by electrospinning for functional textiles. Adv Eng Mater 13(4):356–360
66. Küsgens P, Siegle S, Kaskel S (2009) Crystal growth of the metal–organic framework $Cu_3(BTC)_2$ on the surface of pulp fibers. Adv Eng Mater 11(1–2):93–95
67. O'Neill LD, Zhang H, Bradshaw D (2010) Macro−/microporous MOF composite beads. J Mater Chem 20(27):5720–5726
68. Lykourinou V et al (2011) Immobilization of MP-11 into a mesoporous metal–organic framework, MP-11@mesoMOF: a new platform for enzymatic catalysis. J Am Chem Soc 133(27):10382–10385
69. Drout RJ, Robison L, Farha OK (2019) Catalytic applications of enzymes encapsulated in metal–organic frameworks. Coord Chem Rev 381:151–160

70. Lian X et al (2017) Enzyme–MOF (metal–organic framework) composites. Chem Soc Rev 46 (11):3386–3401
71. Lyu F et al (2014) One-pot synthesis of protein-embedded metal–organic frameworks with enhanced biological activities. Nano Lett 14(10):5761–5765
72. Liang W et al (2019) Enhanced activity of enzymes encapsulated in hydrophilic metal–organic frameworks. J Am Chem Soc 141(6):2348–2355
73. Li P et al (2016) Toward design rules for enzyme immobilization in hierarchical mesoporous metal-organic frameworks. Chem 1(1):154–169
74. Li P et al (2018) Hierarchically engineered mesoporous metal-organic frameworks toward cell-free immobilized enzyme systems. Chem 4(5):1022–1034
75. Liang X et al (2013) From metal–organic framework (MOF) to MOF–polymer composite membrane: enhancement of low-humidity proton conductivity. Chem Sci 4(3):983–992
76. Abbasi Z et al (2017) Simple fabrication of zeolitic imidazolate framework ZIF-8/polymer composite beads by phase inversion method for efficient oil sorption. J Colloid Interface Sci 493:150–161
77. Calvez CL et al (2016) One step synthesis of MOF–polymer composites. RSC Adv 6(21): 17314–17317
78. Siwach P et al (2024) Recent progress in conjugated polymers composites with metal-organic frameworks as electrode materials for supercapacitors. Appl Surf Sci Adv 19:100555
79. Milakin KA et al (2020) Polyaniline-metal organic framework (Fe-BTC) composite for electrochemical applications. Polymer 208:122945
80. Ramos-Fernandez EV et al (2011) MOFs meet monoliths: hierarchical structuring metal organic framework catalysts. Appl Catal A Gen 391(1):261–267
81. Petit C, Bandosz TJ (2009) MOF–graphite oxide composites: combining the uniqueness of graphene layers and metal–organic frameworks. Adv Mater 21(46):4753–4757
82. Petit C, Burress J, Bandosz TJ (2011) The synthesis and characterization of copper-based metal–organic framework/graphite oxide composites. Carbon 49(2):563–572
83. Petit C, Bandosz TJ (2011) Synthesis, characterization, and ammonia adsorption properties of mesoporous metal–organic framework (MIL(Fe))–graphite oxide composites: exploring the limits of materials fabrication. Adv Funct Mater 21(11):2108–2117
84. Górka J et al (2010) Mesoporous metal organic framework–boehmite and silica composites. Chem Commun 46(36):6798–6800
85. Ameloot R et al (2010) Silica–MOF composites as a stationary phase in liquid chromatography. Eur J Inorg Chem 2010(24):3735–3738
86. Kobayashi H, Mitsuka Y, Kitagawa H (2016) Metal nanoparticles covered with a metal–organic framework: from one-pot synthetic methods to synergistic energy storage and conversion functions. Inorg Chem 55(15):7301–7310
87. Chen Y-Z et al (2019) Location determination of metal nanoparticles relative to a metal-organic framework. Nat Commun 10(1):3462
88. Hu S et al (2023) Selectivity control in the direct CO esterification over Pd@UiO-66: the Pd location matters. Angew Chem Int Ed 62(48):e202311625
89. Xu M et al (2021) Interfacial microenvironment modulation boosting electron transfer between metal nanoparticles and MOFs for enhanced photocatalysis. Angew Chem Int Ed 60(30):16372–16376
90. Xiao J-D et al (2016) Boosting photocatalytic hydrogen production of a metal–organic framework decorated with platinum nanoparticles: the platinum location matters. Angew Chem Int Ed 55(32):9389–9393
91. Chen H et al (2019) Electrodeposition of gold nanoparticles on Cu-based metal-organic framework for the electrochemical detection of nitrite. Sensors Actuators B Chem 286:401–407
92. Wen L et al (2023) Electronic state and microenvironment modulation of metal nanoparticles stabilized by MOFs for boosting electrocatalytic nitrogen reduction. Adv Mater 35(15): 2210669

93. Wang H et al (2024) Heteroatom-doped Ag25 nanoclusters encapsulated in metal–organic frameworks for photocatalytic hydrogen production. Angew Chem Int Ed 63(17):e202401443
94. Wen L et al (2024) Hydrophobic microenvironment modulation of Ru nanoparticles in metal–organic frameworks for enhanced electrocatalytic N_2 reduction. Adv Sci 11(34):2405210
95. Wang H et al (2015) Synthesis of an ε-MnO2/metal–organic-framework composite and its electrocatalysis towards oxygen reduction reaction in an alkaline electrolyte. J Mater Chem A 3(31):16168–16176
96. Gao Y et al (2014) The electrochemical performance of SnO2 quantum dots@zeolitic imidazolate frameworks-8 (ZIF-8) composite material for supercapacitors. Mater Lett 128: 208–211
97. Yang J et al (2016) A novel CuxO nanoparticles@ZIF-8 composite derived from core–shell metal–organic frameworks for highly selective electrochemical sensing of hydrogen peroxide. ACS Appl Mater Interfaces 8(31):20407–20414
98. Zafar HK et al (2024) Optimizing electrochemical power generation: harnessing synergies and surface innovation in NiTe-modified MOF nanoarchitectures. J Power Sources 612:234827
99. Dai B et al (2022) Recent advances in carbon nanotube-based biosensors for biomolecular detection. TrAC Trends Anal Chem 154:116658
100. Rani S et al (2020) Sn-MOF@CNT nanocomposite: an efficient electrochemical sensor for detection of hydrogen peroxide. Environ Res 191:110005
101. Shahid M et al (2024) Covalent organic frameworks: synthesis and applications for photocatalysis. ChemPhotoChem 8(10):e202400131
102. Afzal S et al (2024) Recent advances of MXene@MOF composites for catalytic water splitting and wastewater treatment approaches. Chemosphere 364:143194
103. Furukawa S et al (2009) Heterogeneously hybridized porous coordination polymer crystals: fabrication of heterometallic core–shell single crystals with an in-plane rotational epitaxial relationship. Angew Chem Int Ed 48(10):1766–1770
104. Yang J et al (2015) Hollow Zn/Co ZIF particles derived from core–shell ZIF-67@ZIF-8 as selective catalyst for the semi-hydrogenation of acetylene. Angew Chem Int Ed 54(37):10889–10893
105. Gu Y et al (2017) Controllable modular growth of hierarchical MOF-on-MOF architectures. Angew Chem Int Ed 56(49):15658–15662
106. Lee HJ et al (2013) Controlled isotropic or anisotropic nanoscale growth of coordination polymers: formation of hybrid coordination polymer particles. ACS Nano 7(1):491–499
107. Huang H-B et al (2022) Engineering hierarchical architecture of metal-organic frameworks for highly efficient overall CO_2 photoreduction. Small 18(16):2200407
108. Guo C et al (2018) Synthesis of core–shell ZIF-67@co-MOF-74 catalyst with controllable shell thickness and enhanced photocatalytic activity for visible light-driven water oxidation. CrystEngComm 20(47):7659–7665
109. Peng Y et al (2018) Hybridization of MOFs and COFs: a new strategy for construction of MOF@COF Core–Shell hybrid materials. Adv Mater 30(3):1705454
110. Yuan G et al (2022) MOF-COF composite Photocatalysts: design, synthesis, and mechanism. Cryst Growth Des 22(1):893–908
111. Li Y et al (2021) Integration of metal-organic frameworks and covalent organic frameworks: design, synthesis, and applications. Matter 4(7):2230–2265
112. Fan H et al (2021) MOF-in-COF molecular sieving membrane for selective hydrogen separation. Nat Commun 12(1):38
113. Qi K et al (2024) Ultrathin and self-supporting MOF/COF-based composite membranes for hydrogen separation and purification from coke oven gas. Langmuir 40(24):12755–12766
114. Li S et al (2024) Vacuum-assisted confined growth of MOF@COF composite membranes with enhanced hydrogen Permselectivity. Angew Chem Int Ed: 64(7):e202419946